Astronomy
&
Astrophysics

A probable accretion-powered X-ray pulsar in IGR J00370+6122

J. J. M. in 't Zand[1,2], L. Kuiper[1], P. R. den Hartog[1], W. Hermsen[1,3], and R. H. D. Corbet[4,5]

[1] SRON Netherlands Institute for Space Research, Sorbonnelaan 2, 3584 CA Utrecht, The Netherlands
e-mail: jeanz@sron.nl
[2] Astronomical Institute, Utrecht University, PO Box 80000, 3508 TA Utrecht, The Netherlands
[3] Astronomical Institute "Anton Pannekoek", University of Amsterdam, Kruislaan 403, 1098 SJ Amsterdam, The Netherlands
[4] X-ray Astrophysics Laboratory, Code 662, NASA Goddard Space Flight Center, Greenbelt, MD 20771, USA
[5] Universities Space Research Association, USA

ABSTRACT

Serendipitous and dedicated observations with the Rossi X-ray Timing Explorer (RXTE) and the International Gamma-Ray Astrophysics Laboratory (INTEGRAL) were analyzed to study the transient high-mass X-ray binary IGR J00370+6122, in particular to search for an accretion-powered pulsar as companion to the optically identified (Reig et al. 2005, A&A, 440, 637) B0.5 II-III donor star. Highly variable fluxes were measured in the RXTE data during outbursts of up to 2.2×10^{-10} erg cm^{-2} s^{-1} (3–20 keV; averaged over 1 h). During a 1-h time span with RXTE flaring activity was detected with an oscillating signal repeating 7 times. Epoch folding reveals a 346 ± 6 s period. We propose that this is the period of the putative pulsar. This measurement puts the source in the wind-fed accretion region of the $P_{\rm orb}$ (=15.7 d) versus $P_{\rm pulse}$ "Corbet" diagram. The 3 to 60 keV flare spectrum was modeled with an absorbed power law and the absorption column was found to be 15–20 times larger than the interstellar value and the value obtained for the optical counterpart, suggesting an accretor embedded in the wind of the donor star.

Key words. X-rays: binaries – X-rays: individuals: IGR J00370+6122 – X-rays: individuals: 1RXS J003709.6+612131 –
X-rays: individuals 1RXS J003357.9+612645 – accretion, accretion disks – stars: neutron

1. Introduction

The discovery rate of high-mass X-ray binaries (HMXBs) has been high since the launch of the International Gamma-Ray Astrophysics Laboratory (INTEGRAL) in 2002. The known Galactic population has increased by 35% as a result (e.g., Liu et al. 2006). The population now consists of 50% Be X-ray binaries, 25% supergiant X-ray binaries, and 25% peculiar or unknown cases. 60% of all HMXBs are confirmed to contain an accretion-powered pulsar.

The reasons why INTEGRAL has been so effective are its wide field of view and its imaging capability in the hard X-ray band (i.e., 20–100 keV). Thus, INTEGRAL has been able to pick up many so-called "supergiant fast X-ray transients" (SFXTs) and "obscured HMXBs". The latter have such a high absorption due to circumstellar material that study in the traditional 2–10 keV X-ray band is difficult (e.g., Walter et al. 2003; Kuulkers et al. 2005). Some have been optically identified and it has been found that the donors are mostly early spectral-type supergiant stars with massive winds that are responsible for the dense circumstellar medium around the accretor. SFXTs (e.g., Smith et al. 1998; Negueruela et al. 2006; Smith et al. 2006) are not necessarily obscured, but they are transients with such small time scales (hours) that they can only be picked up with instruments with large-enough field of views such as the Imager on Board the INTEGRAL Satellite (IBIS). Possibly clumpy winds are responsible for the brevity of the outbursts (in 't Zand 2005). Both the obscured and fast transient HMXB subclasses had been detected prior to INTEGRAL, but it has been

through INTEGRAL that the large numbers in these populations have come to be realized.

IGR J00370+6122 is one example of an INTEGRAL-discovered HMXB. It was discovered in December 2003 during a 1.2 Ms INTEGRAL observation of the Cassiopeia region (den Hartog et al. 2004; 2006). A ROSAT source in the 2′-radius error region, 1RXS J003709.6+612131, points toward a candidate $V = 9.64$ optical counterpart BD +60 73, an association already suggested by Rutledge et al. (2004). Back-tracking data from the All-Sky Monitor (ASM) on the Rossi X-ray Timing Explorer (RXTE) revealed that IGR J00370+6122 is a recurrent transient whose outbursts recur periodically every 15.665 ± 0.006 d with an average peak flux of 3.3 mCrab (2–12 keV; den Hartog et al. 2004). The periodicity in combination with the optical counterpart suggests IGR J00370+6122 to be a HMXB with an orbital period of 15.665 d. The X-ray modulation points to a significant eccentricity of the orbit or the presence of a circumstellar disk around the donor star.

While Morgan et al. (1955) classified BD +60 73 as a supergiant B1Ib, an analysis of new observations by Reig et al. (2005) points towards a giant B0.5 II-III star without a circumstellar disk (i.e., not a Be star). The photometry points to a distance of 3.0 kpc which is typical for objects in the Perseus arm in the Cassiopeia region.

The aim of our observations was to search for an accretion-powered X-ray pulsar. If detected, this would identify the nature of the accretor as a neutron star. Therefore, we carried out four observations with RXTE, at predicted times of outburst maxima. This many observations were planned, to increase the chance for catching an outburst with a sufficiently high peak flux to be able
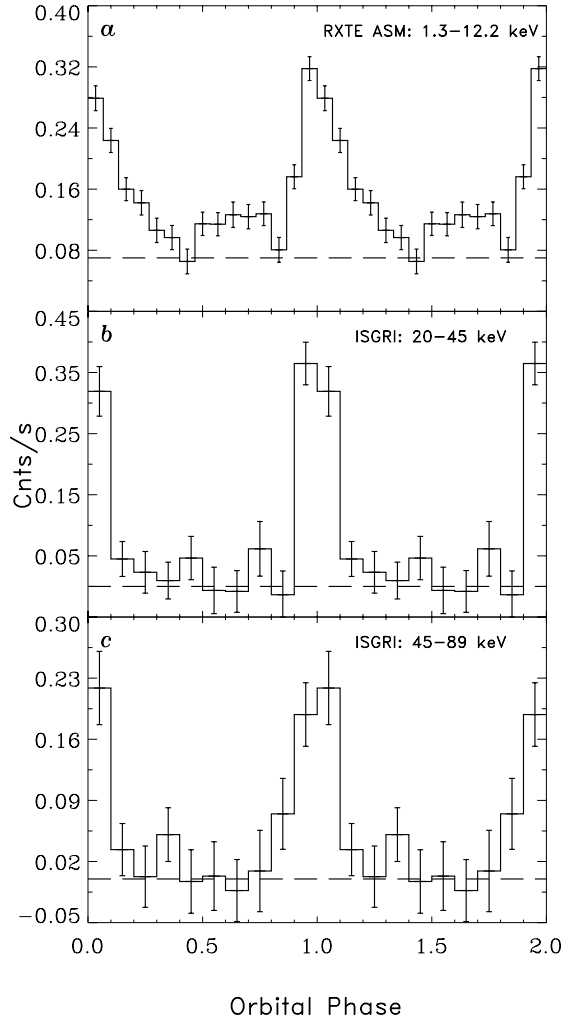
Fig. 1. ASM and INTEGRAL-IBIS-ISGRI light curves folded with $P = 15.6627$ d. The dashes horizontal lines represent the average systematic bias level seen in ASM data (Remillard & Levine 1997) and zero in INTEGRAL data.

to carry out a meaningful study. Furthermore, new observations with the RXTE ASM were analyzed to improve the orbital solution and with INTEGRAL to study the high-energy spectrum.

2. Serendipitous RXTE-ASM, INTEGRAL-IBIS and ROSAT observations

The ASM has been monitoring the X-ray sky since January 1996 in the 2–12 keV bandpass (Levine et al. 1996; Wen et al. 2006). Between Jan. 5, 1996, and Nov. 9, 2006, 64,017 observations were carried out of 90 s each (on average 16 per day; IGR J00370+6122 has a large ecliptic latitude and, therefore, no large ASM data gaps exist due to solar constraints) with an average 1σ sensitivity of 16 mCrab. We infer from these data an ephemeris for the times of maximum flux: $T_{max} =$ MJD 53001.7(3) $+ I \times 15.6627(42)$. This ephemeris is slightly more precise than that published in den Hartog et al. (2004) as quoted in Sect. 1. The folded light curve is presented in Fig. 1 (top panel). The data are of insufficient quality to study this curve at higher spectral resolution.

The INTEGRAL spacecraft (Winkler et al. 2003), launched on 17 October 2002, carries among other instruments the high-angular-resolution imager IBIS (Ubertini et al. 2003). In this

study we only used data recorded by the upper detector system: the INTEGRAL Soft Gamma-Ray Imager ISGRI (Lebrun et al. 2003) which is sensitive between about 20 keV and 1 MeV and has an angular resolution of 12' (full width at half maximum *FWHM*). Its energy resolution of about 7% *FWHM* at 100 keV is amply sufficient to determine the (continuum) spectral properties of hard X-ray sources in the 20 to 300 keV energy band.

In its default operation mode INTEGRAL observes the sky in a dither pattern with $2°$ steps, either rectangular or hexagonal. Typical integration times for each grid point are 1800 to 3600 s. This strategy drives the structure of the INTEGRAL data archive which is organized in about 100 so-called science windows per INTEGRAL orbital revolution (lasting for about 3 days). The INTEGRAL data reduction in this study was performed with the Offline Scientific Analysis (OSA) version 5.1 (Courvoisier et al. 2003; Goldwurm et al. 2003).

The ISGRI data were collected from observations targeted at objects in the Cassiopeia region (i.e., Cas A, Tycho supernova remnant, 4U 0142+61, IGR J00291+5934 and 4U 0115+63) covering the time period between December 12, 2003 and July 7, 2006 (MJD 52985-53920; INTEGRAL revolutions 142 to 454). Only observations with IGR J00370+6122 within $14°.5$ from the pointing axis were included, adding up to a total exposure time of 4.28 Ms in 1536 science windows. This covers data on 11 outbursts from IGR J00370+6122. The ISGRI coverage of 5 outbursts is good, covering well all phases within 0.1 from 0.0. Thus, the combined data should provide a fairly good representation of the average behavior of the outbursts. The ISGRI data were split in 20 logarithmically binned energy bands over the 20–300 keV energy range. For each science window the flux of IGR J00370+6122 was derived for all energy bands using the default IBIS image deconvolution tools in OSA.

The INTEGRAL data are not useful for improving the orbital ephemeris evaluated from ASM data because they stretch over only 2.6 instead of 10.8 yr. However, when folding all INTEGRAL data at a time resolution of 1 science window with the ASM-determined orbital period a significant modulation was found, see Fig. 1 (lower two panels), that lines up with the ASM folded light curve. In the INTEGRAL band the quiescent level extends over almost 0.8 in phase. The 3σ upper limit in the quiescent state is a factor of 11 lower than the peak flux. The ASM data suggest some activity over most of the orbit with fluxes approximately a factor of 10 below the peak flux, but these data are so close to the average systematic bias level seen in ASM data (Remillard & Levine 1997) that we regard the evidence of such activity as inconclusive. The ASM profile is different from those measured with INTEGRAL, suggesting that on average there is spectral softening in the decay phase of the outbursts.

Figure 2 shows the average IBIS spectrum for the 2 phase bins around the peak of the outburst in the folded light curve. The spectrum is satisfactorily described ($\chi_\nu^2 = 1.04$ with $\nu = 11$) by a power law with a photon index of $\Gamma = 1.84 \pm 0.15$. The average 20–80 keV flux is $(4.3 \pm 0.3) \times 10^{-11}$ erg cm^{-2} s^{-1}.

IGR J00370+6122 was covered twice by the ROSAT All-Sky-Survey (Voges et al. 1999), in the time intervals MJD 48281.13-48281.71 and 48472.79-48473.05 with orbital phases 0.61-0.65 and 0.85-0.86 respectively with a 1σ error of 0.02. The signal-to-background count rate ratio was 0.3 ± 0.1 and 11.8 ± 1.6 respectively. Therefore, there is only a detection in the second time interval, consistent with the ephemeris of recurrent outbursts. For an absorbed power law with N_H between 6 and 9×10^{22} cm^{-2} and photon index between 2.1 and 2.5 (see below), the ROSAT PSPC flux translates to a 3–20 keV absorbed
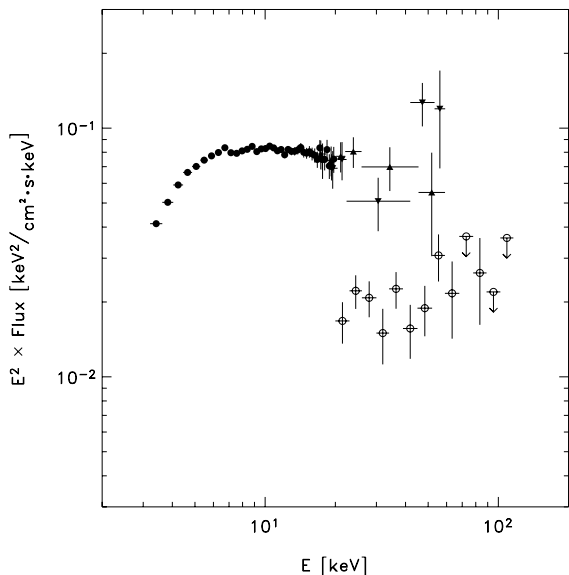
Fig. 2. Average IBIS-ISGRI outburst spectrum (open circles) during orbital phases 0.9–1.1 (cf., Fig. 1) and RXTE spectrum during the flaring state (solid circles indicate PCA measurements, upward pointed triangles HEXTE cluster A measurements and downward pointed triangles HEXTE cluster B measurements).

flux between 0.4 and 5×10^{-9} erg cm^{-2} s^{-1}. This is within an order of magnitude consistent with the highest fluxes measured with RXTE during the flaring (see below).

3. Dedicated RXTE observations

3.1. Observations and light curve

Apart from the ASM, RXTE also carries the Proportional Counter Array (PCA) and the High-Energy X-ray Timing Experiment (HEXTE). The PCA consists of 5 proportional counter units (PCUs) with a total net collecting detector area of 8000 cm^2 in the 2–60 keV band (Jahoda et al. 2006). During any observation any number of PCUs between 1 and 5 are on. The PCA is a non-imaging device with a 2 degree wide field of view (full width to zero response). HEXTE consists of two clusters of four detectors with a total area of 1600 cm^2 in the 10 to 250 keV band (Rothschild et al. 1998). It also is a non-imaging device with the same field of view as the PCA. However, during an observation the two clusters are alternately rocked on and off-source to allow the determination of the background. The rocking mode dwell time for our observations was 32 s.

Recently another X-ray source was reported that is within the fields of view of the PCA and HEXTE during our observations. Kuiper et al. (2006) announced IGR J00335+6126 which is probably associated with a source detected in the ROSAT All-Sky Survey: 1RXS J003357.9+612645. The 20–80 keV flux is $(7.7 \pm 1.2) \times 10^{-12}$ erg cm^{-2} s^{-1}. No variability was observed in excess of 30% when comparing the first half to the second half of the IBIS ISGRI data. The average photon index is $\Gamma = 2.3 \pm 0.6$, comparable to what is measured for IGR J00370+6122. The source is 23.′5 from IGR J00370+6122 and, therefore, contributes up to 60% of its flux to that measured with the PCA or HEXTE when pointed at IGR J00370+6122.

The ephemeris published in den Hartog et al. (2004) was employed to predict outburst times and schedule dedicated RXTE observations. The accuracy of that solution was sufficient for that purpose. A log of the performed RXTE observations is provided

in Table 1, including the orbital phases covered with respect to maximum flux and the average absorbed energy fluxes that we derived from a spectral analysis. The total effective exposure time for the PCA is 44.4 ks after application of the filter criteria as designed for the standard products. Although the flux was always at a level of at least 1×10^{-11} erg cm^{-2} s^{-1} (3–20 keV), it was in one observation (ObsID 91061-01-01-01) at least 4 times higher than in any other and 2 times the peak in the ASM folded light curve. For the weakest measured flux (ObsID 91061-01-02-01) the extrapolated 3–20 keV flux of the contaminating source 1RXS J003357.9+612645 is of a comparable level as the measured flux.

A light curve of all data is provided in Fig. 3. The horizontal line indicates the predicted flux of the contaminating source, ergo the zero flux level of IGR J00370+6122. It is clear that the flux is highly variable, despite the accurate timing with respect to the active phases measured with the ASM (Fig. 1). This shows that the folded ASM light curve merely represents the average behavior, in the sense that accretion only occurs within certain phase limits, but that the level within those limits differs strongly. The statistical quality of the ASM data does not allow the accurate measurement of differences from binary orbit to orbit. A few single outbursts were detected with INTEGRAL and the BeppoSAX Wide Field cameras (den Hartog et al. 2006), with peak fluxes of up to 450×10^{-12} erg cm^{-2} s^{-1} (3–20 keV) averaged over a 0.7 d exposure. This is 5 times the peak of the ASM folded light curve. Furthermore, IGR J00370+6122 is seen to flare on a time scale of an hour, see also Fig. 4. The flux during the flare maximum flux is about 17 times the peak of the ASM folded light curve (see also Sect. 3.3).

For the average flux during the flaring activity (ObsID 91061-01-01-01) the predicted contribution from the contaminating source is less than 5% of the measured flux. One could contest that the flare is due to the contaminating source instead of IGR J00370+6122. However, we believe this is unlikely because IGR J00370+6122 was targeted at its known outburst times and it would be an unlikely coincidence if the other source would flare at the same time (note that the ASM and INTEGRAL have sufficient angular resolution to distinguish both sources). The contaminating source is neglected in our discussion of the flare spectrum. The contamination may be more serious in the "non-flaring" observations.

3.2. PCA timing analysis

The PCA data are best suited for a timing analysis since the HEXTE photon count rate is an order of magnitude smaller. Figure 4 zooms in on the PCA data of the flaring state. The flaring appears to be fully contained in the 4032 s long observation: there is no flaring at the start nor end of the observation. Most interestingly, there is a strong suggestion of a periodicity in the flux during the flare which is mangled by a simultaneously strongly varying flux. The period is close to 340 s. For such a period, the modulation profile consists of a primary peak which is repeated 7 or 8 times and a secondary intermediate peak which only appears 4 times at the largest flux levels. To investigate the periodicity further Standard-1 data were extracted which have a resolution of 1/8 s with all detectors and channels combined. Times were corrected to the solar system barycenter. Figure 5 shows the periodogram for a selection of the data taken between 500 and 3700 s after the observation start. There are three peaks, at about 340, 550 and 700 s. The latter may be the 1:2 subharmonic of the peak at 340 s. The peak at 340 s is most coherent. Its relative width of 0.1 is roughly as expected for a coherent signal (i.e., the

Table 1. Observation log and basic parameters. The on-target time was calculated with the filter criteria from the standard products and applies to the PCA. The actual time is 20% larger. Flux and photon index Γ are without subtraction of the contamination of IGR J00335+6126. Flux is in units of 10^{-12} erg cm^{-2} s^{-1} within 3–20 keV and is not corrected for absorption. N_H is in units of 10^{22} cm^{-2}. Errors are 1σ, upper limits are for 90% confidence.

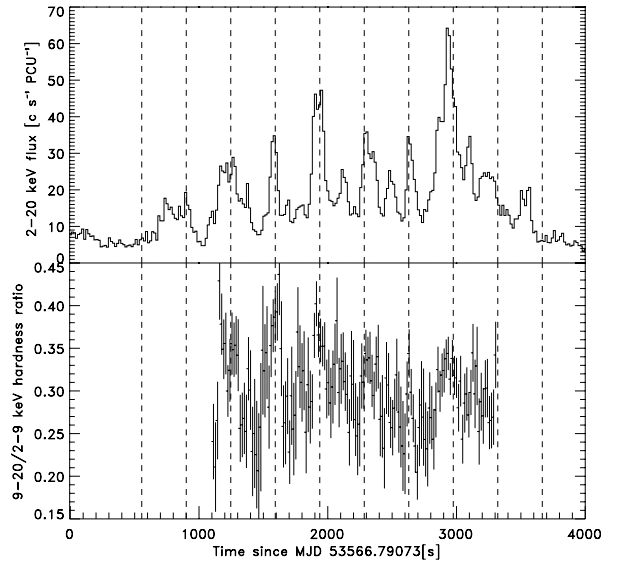| Observation ID	Active PCUs	Dates (MJD)	On-target time (s)	Orbital phase	Flux	Γ	N_H
90415-01-01-00	0, 1, 2, 3	53144.90093–53144.91130	928	0.141–0.142	11	3.25 ± 0.40	7.5 ± 3.7
90415-01-02-00	0, 2, 3	53158.77685–53158.82130	3728	0.027–0.030	14	2.96 ± 0.22	7.9 ± 2.3
91061-01-01-00	0, 2, 3	53566.59963–53566.75056	8864	0.061–0.071	21	2.54 ± 0.05	10.2 ± 0.8
91061-01-01-01	0, 2, 3	53566.78574–53566.84796	4032	0.073–0.077	220	2.14 ± 0.02	9.1 ± 0.3
91061-01-02-01	0,2	53581.78519–53581.80000	1088	0.031–0.032	12	2.45 ± 0.65	<12
91061-01-02-02	0, 1, 2, 3	53581.83593–53581.86704	2368	0.034–0.036	19	3.46 ± 0.18	9.7 ± 1.7
91061-01-02-00	0, 2, 3, 4/0, 1, 2/0, 2	53581.91574–53582.13907	9264	0.039–0.053	21	3.06 ± 0.14	7.6 ± 1.5
91061-01-03-00	0, 1, 2/0, 2, 4/0, 2, 3	53597.55500–53597.83907	14160	0.037–0.055	56	2.47 ± 0.05	6.3 ± 0.6
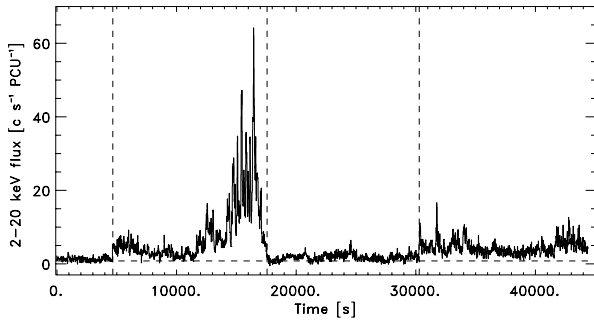
Fig. 3. "Sandwiched" background-subtracted light curve in 2–40 keV. All data gaps have been eliminated. The positions of the major data gaps have been indicated with vertical dashed lines; they are equivalent to the division lines in Table 1. The horizontal dashed line indicates the most probable flux of the contaminating source and, thus, represents a zero line for the flux from IGR J00370+6122.

Fig. 4. (*Top*) 2–20 keV background-subtracted light curve of IGR J00370+6122 with the PCA during the flaring state. The dashed lines serve as a guide for a 346 s periodicity. (*Bottom*) Spectral hardness evolution during brightest parts.

expected full width at half maximum for a coherent sinusoidal signal is $\Delta P/P = 1/2N$ with $n = \delta T/P$ the number of periods P within the time stretch δT). The period was determined by fitting a quadratic function within 10 s from the relevant peak: 345.7 s. The statistical error inferred from the peak χ^2 value following Leahy (1987) is 2.3 s. However, the strongly changing flux level introduces systematic errors. We find from Monte Carlo simulations that the period inferred from epoch folding systematically differs by 5 s between the situation when the average flux level from pulse to pulse is constant or when it follows a Gaussian-shaped function centered at the middle of the observation and with a *FWHM* of 1500 s. Combining the statistical and systematic errors quadratically, a period measurement was derived of 346 ± 6 s.

The evidence for a periodicity in these data is very suggestive but not conclusive. This is due to the brevity of the flare, as compared to the period. In none of the other PCA data could a periodic signal be found. The INTEGRAL data are not suitable for a meaningful search. The combined significance is 13.6σ, and a 3σ detection limit for a periodic modulation is equivalent to an amplitude of approximately 60% for an 8-bin phase resolution, assuming that the signal is present at all times. This amplitude limit is close to what was measured with the PCA during the flare.

It appears that the mass accretion rate is varying so quickly that there is no opportunity to develop a stable pulsar signal. Still, we propose that the 346 s period signal is the putative pulsar. The peak in the periodogram is narrowest, indicative of the strongest coherence, and the light curve shows this periodicity

quite obviously. Unfortunately, the small endurance of the pulse signal with respect to the orbital period and the accuracy of the measurement is insufficient to pursue orbital parameters other than the period.

We also studied the data at higher time resolution, through the average Fourier power density spectrum of all 16 s data stretches during the flaring (i.e., all data in ObsID 91061-01-01-01). No coherent signals were found between 1 ms and 1 s with a 95% confidence upper limit on the amplitude of 13% fractional rms.

3.3. Spectral analysis

The PCA (between 3 and 20 keV) and HEXTE spectrum (between 15 and 60 keV) were modeled with an absorbed power law. The results are presented in Table 1 with a resolution of one ObsID. The spectra outside the flare are likely severely contaminated by 1RXS J003357.9+612645 and were ignored. The average spectrum during the flare is characterized by $N_H = (9.1 \pm 0.3) \times 10^{22}$ cm^{-2}, a photon index of $\Gamma = 2.14 \pm 0.02$ and an absorbed 3–20 keV flux of $(2.2 \pm 0.1) \times 10^{-10}$ erg cm^{-2} s^{-1} $(3.5 \times 10^{-10}$ erg cm^{-2} s^{-1} in 3–60 keV). The reduced χ^2 is an acceptable 1.19 (81 d.o.f.). The unabsorbed flux for this
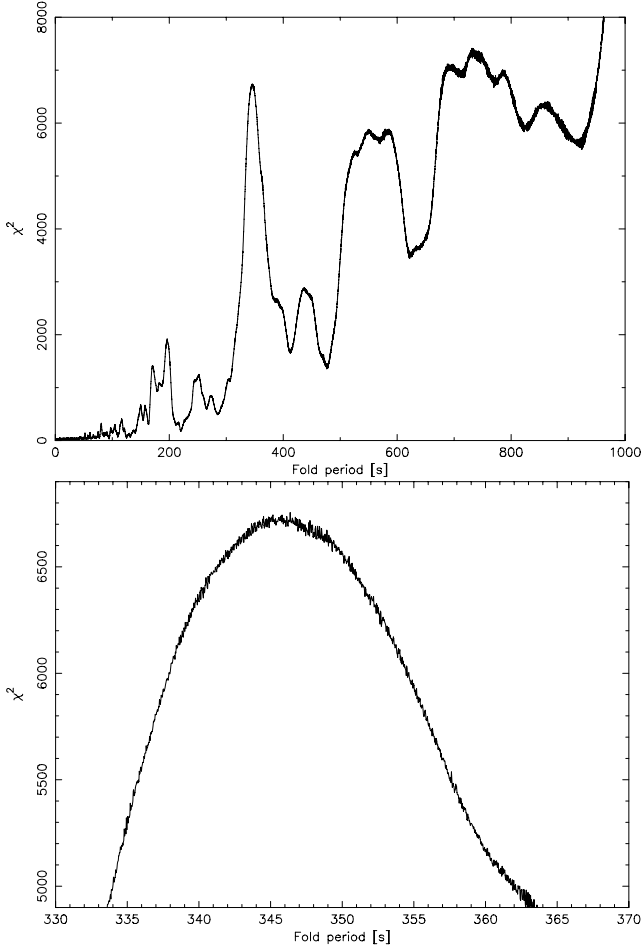
Fig. 5. Periodogram of standard-1 data for the interval 500 and 3700 s in Fig. 4. The bottom figure is a zoomed-in part of the top figure. The applied phase resolution was 1/32.

model is 2.8×10^{-10} erg cm^{-2} s^{-1} (4.1×10^{-10} erg cm^{-2} s^{-1} in 3–60 keV). For a distance of 3 kpc this translates to a luminosity of 4×10^{35} erg s^{-1}. During the peak this may be as high as 3×10^{36} erg s^{-1}.

Figure 2 shows the RXTE flare spectrum in relation to the average IBIS outburst spectrum. It illustrates an order of magnitude flux difference. There are INTEGRAL data taken simultaneous with the RXTE data of the flare, but they suffered from increased background levels due to a large solar flare and were not constraining.

The hydrogen column density is 15–20 times higher than the interstellar medium measurements following the HI map by Dickey & Lockman (1990) and the value implied (Predehl & Schmitt 1995) by $E(B - V) = 0.78$ determined for the optical counterpart by Reig et al. (2005). The fact that the optical counterpart is not affected by the high absorption suggests that the accretor is situated in the focused wind from the donor star. The absorption is consistent with previous measurements (cf., den Hartog et al. 2006) and not variable beyond approximately 20%.

As the hardness ratio shows in Fig. 4, the spectrum tends to harden with flux. This is not unexpected for a pulsar signal (e.g., Robba et al. 2001; La Barbera et al. 2003, 2005)

4. Discussion

The new findings on IGR J00370+6122 presented here are the likely detection of the pulsar and the flaring behavior. The tentative $P_{\rm pulse}$ measurement and the firm $P_{\rm orb}$ measurement places IGR J00370+6122 in the wind-accretion regime of the Corbet diagram of HMXBs (Corbet 1986). Most of the wind-accreting systems have a supergiant donor, but IGR J00370+6122 does not (Reig et al. 2005). In this respect it bears resemblance to the transient source SAX J2103.5+4545 ($P_{\rm orb} = 12.6$ d, $P_{\rm pulse} = 359$ s, Hulleman et al. 1998; Baykal et al. 2000), which also resides in the wind-accretion regime but has a B0V/B0Ve donor (Reig et al. 2004, 2005). Reig et al. have made multiple optical measurements of SAX J2103.5+4545 and find a disappearance of the emission lines and, ergo, the circumstellar disk, while the X-ray source remains active which would then make it a wind accretor. This shows that at a detailed level, spectral classification of HMXB donors may change as a result of changes in the wind. This could also be happening to IGR J00370+6122. It makes sense to perform multiple spectroscopic observations.

Flaring is a common feature in HMXBs, particularly in wind-fed systems, see for instance in GX 301-2 (e.g., Koh et al. 1997), 4U 1700-37 (e.g., Boroson et al. 2003) and Vela X-1 (e.g., Staubert et al. 2004). This flaring is probably related to inhomogeneities in the circumstellar material being accreted or accretion instabilities. In HMXBs with an accretion disk (Roche-lobe overflow systems and many Be X-ray binaries), the accretion rate is smoothed and flares are not that common. This is in line with a wind-fed accretion in IGR J00370+6122. We note that the flaring is not quite the same phenomenon as in SFXTs because the dynamic range of the flux change in IGR J00370+6122 (a factor of $\sim$10) is much smaller than in SFXTs ($>10^3$; e.g., Sakano et al. 2002 and in 't Zand 2005).

$N_{\rm H}$ is a factor of 15–20 higher than the interstellar value (Dickey & Lockman 1990) and that implied by the color excess $E(B - V)$ of the optical counterpart. Its absolute value of 9×10^{22} cm^{-2} is close to the threshold value for obscured sources of 10^{23} cm^{-2}. This suggests that the accretor is embedded in a dense part of the wind from the donor star.

The recurrent transient nature points to a large eccentricity of the 16 d orbit. For about 80% of the orbit, the NS is probably traversing a low-density part of the wind and accretion is centrifugally inhibited. Only when it moves closer to the donor, denser parts are traversed and the inhibition is overcome. Determination of orbital parameters, such as eccentricity and periastron distance, would be able to test this hypothesis, but this may prove difficult. X-ray pulsar timing is difficult due to the transient signal and studies of radial velocity curves from optical spectra is difficult due to small amplitudes (of order 10 km s^{-1}) and complications of this method in general with HMXBs (e.g., Barziv et al. 2001). The hope is that the source may in the future exhibit a prolonged period of accretion due to an enhanced wind from the donor.

References

Barziv, O., Kaper, L., van Kerkwijk, M. H., Telting, J. H., & van Paradijs, J. 2001, A&A, 377, 925
Baykal, A., Stark, M. J., & Swank, J. 2000, ApJ, 544, L129
Boroson, B., Vrtilek, S., Kallman, T., & Corcoran, M. 2003, ApJ, 592, 516
Corbet, R. H. D. 1986, MNRAS, 220, 1047
Courvoisier, T. J.-L., Walter, R., Beckmann, V., et al. 2003, A&A, 411, L53
Dickey, J. M., & Lockman, F. J. 1990, ARA&A, 28, 215
den Hartog, P. R., Kuiper, L. M., Corbet, R. H. D., et al. 2004, ATel, 281
den Hartog, P. R., Hermsen, W., Kuiper, L., et al. 2006, A&A, 451, 587
Goldwurm, A., David, P., Foschini, L., et al. 2003, A&A, 411, L223
Hulleman, F., in 't Zand, J. J. M., & Heise, J. 1998, A&A, 337, L25
in 't Zand, J. J. M. 2005, A&A, 441, L1
Jahoda, K., Markwardt, C. B., Raveda, Y., et al. 2006, ApJS, 163, 401
Koh, D., Bildsten, L., Chakrabarty, D., et al. 1997, ApJ, 479, 933
Kuiper, L. M., den Hartog, P. R., & Hermsen, W. H. 2006, ATel, 939
Kuulkers, E. 2005, in Interacting Binaries: Accretion, Evolution, and Outcomes, ed. L. Burderi, et al., AIP Conf. Proc., 797, 402
La Barbera, A., Santangelo, A., Orlandini, M., & Segreto, A. 2003, A&A, 400, 993
La Barbera, A., Segreto, A., Santangelo, A., Kreykenbohm, I., & Orlandini, M. 2005, A&A, 438, 617
Lebrun, F., Leray, J. P., Lavocat, P., et al. 2003, A&A, 411, L141
Leahy, D. A. 1987, A&A, 180, 275
Levine, A., Bradt, H., Cui, W., et al. 1996, ApJ, 469, L33
Liu, Q. Z., van Paradijs, J., & van den Heuvel, E. P. J. 2006, A&A, 455, 1165

Morgan, W. W., Code, A. D., & Whitford, A. E. 1955, ApJS, 2, 41
Negueruela, I., Smith, D. M., Reig, P., Chaty, S., & Torrejon, J. M. 2006, in Proc. The X-ray Universe 2005, ed. A. Wilson, ESA SP-604 (Noordwijk: ESA Pub. Div.), 165
Predehl, P., & Schmitt, J. H. M. M. 1995, A&A, 293, 889
Reig, P., Negueruela, I., Frabregat, J., et al. 2004, A&A, 421, 673
Reig, P., Negueruela, I., Papamastorakis, G., Manousakis, A., & Kougentakis, T. 2005, A&A, 440, 637
Remillard, R. A., & Levine, A. M. 1997, in Proc. All-Sky X-Ray Observations in the Next Decade, ed. M. Matsuoka, & N. Kawai, 29
Robba, N. R., Burderi, L., Di Salvo, T., Iaria, R., & Cusumano, G. 2001, ApJ, 562, 950
Rothschild, R. E., Blanco, P. R., Gruber, D. E., et al. 1998, ApJ, 496, 538
Rutledge, R. E. 2004, ATel, 282
Sakano, M., Koyama, K., Murakami, H., Maeda, Y., & Yamauchi, S. 2002, ApJS, 138, 19
Smith, D. M., Main, D., Marshall, F., et al. 1998, ApJ, 501, L181
Smith, D. M., Heindl, W. A., Markwardt, C. B., et al. 2006, ApJ, 638, 974
Staubert, R., Kreykenbohm, I., Kretschmar, P., et al. 2004, Proc. 5th Workshop on the INTEGRAL Universe, ed. V. Schönfelder, G. Lichti, & C. Winkler, ESA SP-552, 259
Voges, W., Ashenbach, B., Boller, Th., et al. 1999, A&A, 349, 389
Ubertini, P., Lebrun, F., Di Cocco, G., et al. 2003, A&A, 411, L131
Walter, R., Rodriguez, J., Foschini, L., et al. 2003, A&A, 411, L427
Wen, L., Levine, A., Corbet, R. H. D., & Bradt, H. V. 2006, ApJS, 163, 372
Winkler, C., Courvoisier, T. J.-L., Di Cocco, G., et al. 2003, A&A, 411, L1